Molecular Vision 2018; 24:834-846 <http://www.molvis.org/molvis/v24/834>
Received 25 April 2018 | Accepted 28 December 2018 | Published 30 December 2018

Rescue of cone function in cone-only *Nphp5* knockout mouse model with Leber congenital amaurosis phenotype

Christin Hanke-Gogokhia,[1] Vince A. Chiodo,[2] William W. Hauswirth,[2] Jeanne M. Frederick,[1] Wolfgang Baehr[1,3,4]

[1]Department of Ophthalmology, John A. Moran Eye Center, University of Utah Health Science Center, Salt Lake City, UT; [2]Department of Ophthalmology, University of Florida, Gainesville, FL; [3]Department of Neurobiology and Anatomy, University of Utah Health Science Center, Salt Lake City, UT; [4]Department of Biology, University of Utah, Salt Lake City, UT

Purpose: Recessive mutations in the human *IQCB1/NPHP5* gene are associated with Senior-Løken syndrome (SLS), a ciliopathy presenting with nephronophthisis and Leber congenital amaurosis (LCA). *Nphp5*-knockout mice develop LCA without nephronophthisis. Mutant rods rapidly degenerate while mutant cones survive for months. The purpose of this study was to reinitiate cone ciliogenesis in a *Nphp5*$^{-/-}$; *Nrl*$^{-/-}$ mouse with viral expression of full-length NPHP5 and rescue function.

Methods: *Nphp5*$^{-/-}$ mice were mated with *Nrl*$^{-/-}$ mice to generate *Nphp5*$^{-/-}$; *Nrl*$^{-/-}$ double-knockouts. *Nphp5*$^{-/-}$; *Nrl*$^{-/-}$ mice and *Nphp5*$^{+/-}$; *Nrl*$^{-/-}$ controls were phenotyped with confocal microscopy from postnatal day 10 (P10) until 6 months of age. *Nphp5*$^{-/-}$; *Nrl*$^{-/-}$ mice and *Nphp5*$^{+/-}$; *Nrl*$^{-/-}$ controls were injected at P15 with self-complementary adenoassociated virus 8 (Y733F) (AAV8(Y733F)) expressing GRK1-FL-cNPHP5. Expression of mutant NPHP5 was verified with confocal microscopy and electroretinography (ERG).

Results: In the *Nphp5*$^{-/-}$ and cone-only *Nphp5*$^{-/-}$; *Nrl*$^{-/-}$ mice, cone outer segments did not form, but mutant cones continued to express cone pigments in the inner segments without obvious signs of cone cell death. The mutant cone outer nuclear layer (ONL) and the inner segments were stable for more than 6 months in the cone-only *Nphp5*$^{-/-}$; *Nrl*$^{-/-}$ retinas. Viral expression of NPHP5 initiated after eye opening showed that connecting cilia and RP1-positive axonemes were formed. Furthermore, cone pigments and other cone outer segment proteins (cone transducin and cone PDE6) were present in the nascent mutant cone outer segments, and rescued mutant cones exhibited a significant photopic b-wave (30% of *Nphp5*$^{+/-}$; *Nrl*$^{-/-}$ controls).

Conclusions: *Nphp5*$^{-/-}$; *Nrl*$^{-/-}$ cones persistently express cone pigments in the inner segments without obvious degeneration, providing an extended duration interval for viral gene expression. Viral expression of full-length NPHP5 initiates ciliogenesis between P15 and P60, and mutant cones are, in part, functional, encouraging future retina gene replacement therapy.

Nephrocystins (NPHP1–18) are a large group of proteins expressed in renal epithelia and other ciliated cells, including photoreceptors. NPHP polypeptides are highly conserved among invertebrate (*Chlamydomonas reinhardtii* and *Caenorhabditis elegans)* and mammalian primary cilia and localize to the basal body and transition zones [1-4]. In renal epithelia, NPHP1, -4, -5, -6, and -8 are present in the transition zone (TZ), whereas NPHP2, -3, and -9 localize to the adjacent Inversin (Inv) compartment [2]. Mutations in nephrocystin genes are associated with several syndromic ciliopathies, including Joubert [5-10], Senior-Løken [11-13], Meckel [14-17], Cogan, and Bardet-Biedl syndromes [18-20]. NPHP1 [21], NPHP4 [22], IQCB1/NPHP5 [23], CEP290/NPHP6 [24-26], SDCCAG8/NPHP10 [27,28], and TMEM67/NPHP11 (meckelin) [29] are known to be associated with retinal degeneration. Mutations in the *IQCB1/NPHP5* gene (OMIM 609237) are the most common cause of Senior-Løken syndrome (SLS) in humans [30,31].

SLS is an autosomal recessive retina-renal ciliopathy characterized by photoreceptor dysfunction and progressive degeneration, accompanied by nephronophthisis (NPHP) [32,33]. The retina degeneration usually resembles retinitis pigmentosa (RP) [34] or Leber congenital amaurosis (LCA) [35]. LCA and RP are characterized by the presence of nonfunctional rods and cones at birth or early in life and progressive loss of rod photoreceptors, respectively [34]. NPHP presents with diminished kidney size, corticomedullary cysts, and tubulointerstitial fibrosis [33]. Most mutations in the human *IQCB1* gene are stop codons or frameshift mutations truncating NPHP5. The retina phenotype of NPHP5-LCA is severe, as the outer nuclear layer (ONL)

Correspondence to: Wolfgang Baehr, Department of Ophthalmology and Visual Sciences, University of Utah Health Science Center, Salt Lake City, UT, 84132; Phone: (801) 585-6643; FAX: (801) 587-7686; email: wbaehr@hsc.utah.edu.
Dr. Christin Hanke-Gogokhia is now at the Dyson Vision Research Institute, Weill Cornell Medical College, 1300 York Avenue, New York, NY, 10065.

is barely detectable in young patients [36]. Surprisingly, nonfunctional cones and cone nuclei are retained at the fovea suggesting that the mutant retina may provide a large window for gene therapy. Mutations in *NPHP5* have also been identified in patients with non-syndromic LCA [23,31] and in naturally occurring animal models [37,38].

Human, mouse, and canine NPHP5 each consist of 598 amino acids and are 90% identical without gaps. NPHP5 polypeptides contain BBSome interaction sites, IQ calmodulin binding motifs, coiled-coil domains, and a C-terminal CEP290 binding site [32,39,40]. The function of NPHP5 is unknown. Germline *Nphp5*-knockout mice, deleting exons 5–15 and removing most IQ and coiled-coil domains, are blind at eye opening exhibiting LCA [30], a phenotype that recapitulates the human pathology of rapid retinal degeneration. *Nphp5*$^{-/-}$ mice do not develop nephronophthisis even at 1 year of age suggesting non-syndromic ciliopathy, perhaps caused by nephrocystin redundancy in kidneys. Basal bodies in *Nphp5*$^{-/-}$ photoreceptors dock to the cell membrane, but fully developed transition zones do not form, and outer segments fail to develop. Ultrastructure of postnatal day (P6) and P10 *Nphp5*$^{-/-}$ photoreceptors reveal aberrant transition zones of reduced diameter.

We generated *Nphp5*$^{-/-}$*; Nrl*$^{-/-}$ double-knockout mice to study the cone degeneration rate and to explore the duration of any window for future gene therapy experiments. We found that although in *Nphp5*$^{-/-}$*; Nrl*$^{-/-}$ mice cone outer segments do not form, the mutant cone outer nuclear layer is stable up to 6 months of age. Mutant cones continued to express cone pigments in the inner segments, axons, and endoplasmic reticulum surrounding nuclei, without recognizable degeneration. Employing self-complementary adenoassociated virus 8 (scAAV8) vectors, we expressed canine NPHP5 (cNPHP5) to test whether ciliogenesis and the formation of the outer segments may be reinitiated postnatally. The results show that functional axonemes and outer segments form in part upon delivery of scAAV8 expressing NPHP5. Moreover, cone phototransduction proteins localize normally to the outer segments, and mutant cones respond to light.

METHODS

Animals: Procedures were approved by the University of Utah Institutional Animal Care and Use Committee and were conducted in compliance with the NIH Guide for Care and Use of Laboratory Animals. The protocol was approved by the University of Utah Animal Care and Use Committee, and all animals were treated according to the ARVO Statement for the Use of Animals in Ophthalmic and Vision Research. *Nphp5* mutant animals were previously generated in our laboratory [30] and maintained in a 12 h:12 h light-dark cycle. An *Nrl*$^{-/-}$ mouse (JAX stock # 021,152) was used to generate the cone-only retina. A transgenic mouse expressing EGFP-CETN2 fusion protein (JAX stock # 008,234) was used to identify the centrioles and transition zones with fluorescence microscopy [41].

Generation and genotyping of Nphp5/Nrl double-knockout mice: Nphp5$^{-/-}$ male mice were bred with *Nrl*$^{-/-}$ female mice to generate *Nphp5*$^{+/-}$*; Nrl*$^{+/-}$ double heterozygotes. Male and female *Nphp5*$^{+/-}$*; Nrl*$^{+/-}$ mice were bred to generate double-knockouts. *Nphp5*$^{-/-}$ mice and *Nrl*$^{-/-}$ mice were genotyped (Figure 1A) as described [30,42]. *Nphp5* mutant animals were genotyped using primers *Nphp5F* (5'-CCT TTA GGG TGA TAG TAG CCA ATT CC), *Nphp5Rw* (5'-AGG AAC TAA GCT GTG AAA TGG ACC) and *Nphp5mut* (5'-CAA CGG GTT CTT CTG TTA GTC C). The WT allele yields an amplicon of 452 bp; mutant allele, 294 bp. The *Nrl* allele was detected by amplification of a 607-bp fragment of Nrl exon 3 (forward primer, 5′–GCT GGT CTC GAT GTC TGT–3′; reverse, 5′–CAT TCA GCA TGC CAC CTG–3′).

Immunohistochemistry: Animals were dark-adapted overnight and euthanized by cervical dislocation under dim red light. Dissection of the eyecups and retina cryosections for confocal microscopy were prepared as described [43]. Briefly, sections were incubated with the following polyclonal primary antibodies: anti-M/L-opsin (1:500; Chemicon, Fisher Scientific, Salt lake City, UT), anti-S-opsin (1:500; Chemicon), anti-RP1 (1:1,000, a generous gift from Drs. Qin Liu and Eric Pierce, Harvard), anti-cone PDE6 (cPDE6, 1:500, a generous gift from Dr. Tiansen Li, NEI), anti-cone-transducin-α (anti-cone Tα, 1:500; Santa Cruz, Dallas, TX), and anti-cone-transducin-γ (anti-cone Tγ, 1:500; Cytosignal). Monoclonal antibodies included anti-Flag (1:100, Sigma). Secondary antibodies Alexa Fluor 555-conjugated goat-anti-rabbit, Alexa Fluor 555-conjugated goat-anti-mouse, and Alexa Fluor 555-conjugated goat-anti-chicken were diluted 1:1,000 in blocking solution (2% bovine serum albumin [BSA], 0.1% Triton X-100, 0.1 M phosphate buffer pH 7.4). Images were acquired using a Zeiss LSM800 confocal microscope.

Electroretinography: Photopic electroretinogram (ERG) responses were recorded from 2-month-old *Nphp5*$^{+/-}$*; Nrl*$^{-/-}$ and *Nphp5*$^{-/-}$*; Nrl*$^{-/-}$ mice using a UTAS BigShot Ganzfeld system (LKC Technologies, Gaithersburg, MD). ERGs were measured as described [44,45]. Briefly, mice were light-adapted under a background light of 1.48 log cd s·m^{-2} for 5–10 min. Single-flash responses of treated and untreated eyes were recorded at stimulus intensities of −1.6 log cd·s·m^{-2} to 2.4 log cd·s·m^{-2}.

Figure 1
Hanke-Gogokhia et al.

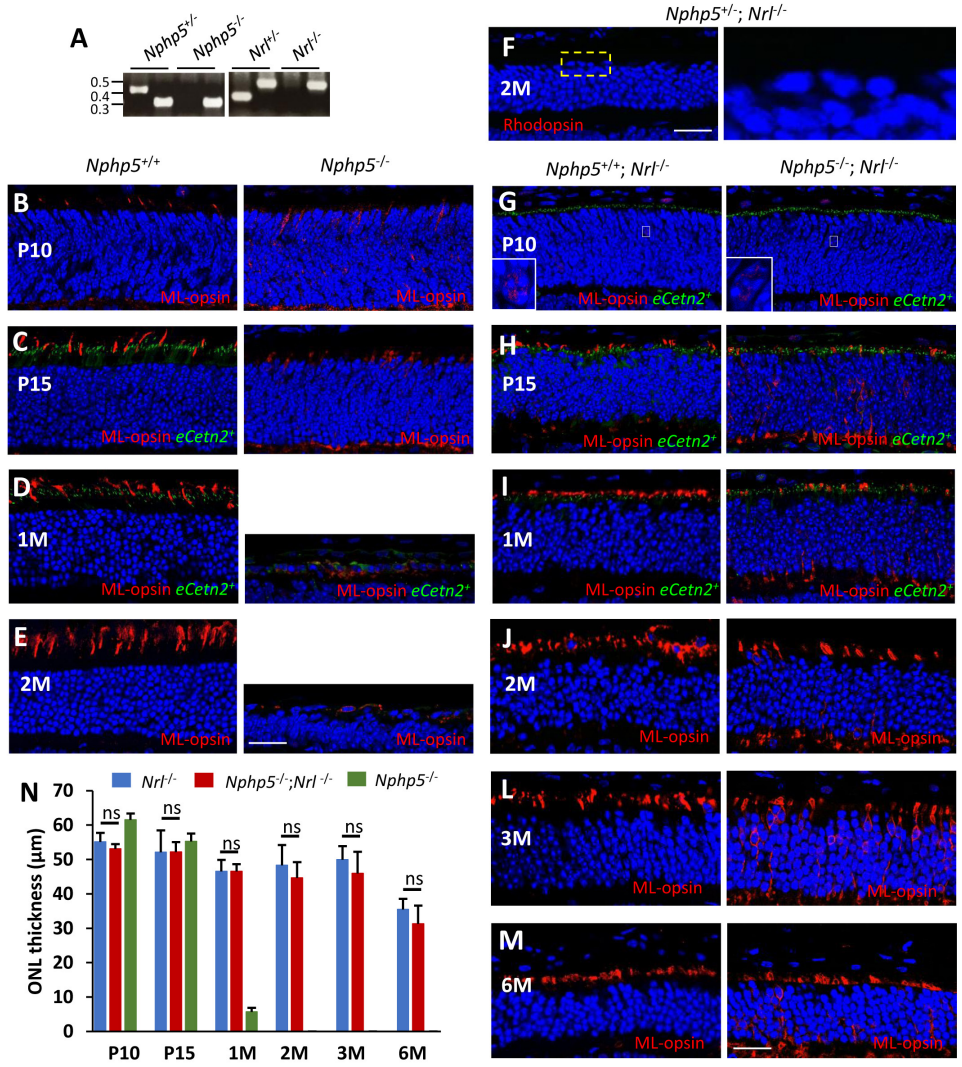

Figure 1. Phenotyping *Nphp5* and *Nphp5; Nrl* double-knockout mice. **A**: Genotyping of *Nphp5* and *Nrl* alleles. **B**–**E**: Expression of ML-opsin (red) in *Nphp5*$^{+/+}$ (left panels) and *Nphp5*$^{-/-}$ cones (right panels) at P10 (**B**), P15 (**C**), 1 month (**D**), and 2 months (**E**) in the presence of *Egfp-Cetn2*$^{+}$ (**C**, **D**). **F**: Absence of rhodopsin in the *Nphp5*$^{+/-}$; *Nrl*$^{-/-}$ retina. **G**–**M**: Expression of ML-opsin in *Nphp5*$^{+/+}$; *Nrl*$^{-/-}$ (left panels) and *Nphp5*$^{-/-}$; *Nrl*$^{-/-}$ cones (right panels) at P10 (**G**), P15 (**H**), 1 month (**I**), 2 months (**J**), 3 months (**L**), and 6 months (**M**). *Egfp-Cetn2*$^{+}$ (*eCetn2*$^{+}$, green) identifies the centrioles and transition zones. Nuclei are contrasted using 4′,6-diamidino-2-phenylindole (DAPI, blue). Scale bar, 20 µm. **N**: ONL thickness of *Nrl*$^{-/-}$, *Nphp5*$^{-/-}$, and *Nphp5*$^{-/-}$; *Nrl*$^{-/-}$ retinas (n=3) as a function of time. The deterioration of the double-knockout ONL relative to the *Nrl*$^{-/-}$ control is not statistically significant. OS, outer segment; IS, inner segment; ONL, outer nuclear layer; P, postnatal day; M, month.

scAAV8-cNPHP5 virus production and injection: Canine NPHP5 (cNPHP5) expression cassette with an N-terminal Flag tag under the control of the human G-protein-coupled receptor kinase (hGRK1) promoter was packaged into self-complementary AAV2/8 (Y733F;P4211) virus particles as described [46,47]. scAAV8-cNPHP5 virus (1 µl of virus with a titer of 2.27E+12) was injected subretinally shortly after eye opening, between P12 and P15, in the right eye (the treated eye). The left eye was used as the untreated control eye. A total of five of each mutant and control mice were used for virus injection. Eyes were harvested at 2 months of age (approximately 6 weeks post-injection) and evaluated with immunohistochemistry and ERG for retinal rescue.

Statistical analysis: SigmaPlot12 was used for statistical analysis using Student *t* test and F test (ANOVA). A p value of 0.05 was considered statistically significant.

RESULTS

Prolonged survival of cones in the Nphp5$^{-/-}$; Nrl$^{-/-}$ double-knockout retina: Nphp5$^{-/-}$ germline knockout mice recapitulate the human pathology of rapid retinal degeneration mimicking an LCA phenotype [30]. During postnatal development of the photoreceptors, the absence of NPHP5 did not prevent proper anchoring of the basal body to the cell cortex, but the transition zone (the connecting cilium) did not form properly, and rod and cone outer segments were absent [30]. We followed the fate of the cones in the *Nphp5$^{-/-}$* retina in more detail (Figure 1B–E). ML-opsin is expressed in *Nphp5$^{+/+}$* controls at P10 (Figure 1B, left panel) and is present in cone outer segments (COS), while ML-opsin accumulates in the IS and the ONL of *Nphp5$^{-/-}$* cones (Figure 1B, right panel). At P15, COS are near-normal length in the control mice but absent in the single-knockout mice (Figure 1C). At 1 month of age, the *Nphp5$^{-/-}$* ONL is reduced to a single layer of nuclei, presumably cones, as ML-opsin is still present around the nuclei of cell remnants (Figure 1D, right panel). A single nuclear layer is still partly retained at 2 months (Figure 1E, right panel) suggesting that cones may survive longer than rods. The degeneration of *Nphp5$^{-/-}$* rod photoreceptors is complete at 1 month of age (Figure 1D,N).

We generated *Nphp5$^{-/-}$; Nrl$^{-/-}$* double-knockout mice. We confirmed that rods and rhodopsin are absent in cone-only retinas (Figure 1F, shown for the heterozygous control). In the *Nphp5$^{-/-}$; Nrl$^{-/-}$* mutant mice and the *Nphp5$^{+/+}$; Nrl$^{-/-}$* control mice, cone outer segments are undetectable at P10, and ML-opsin appears to accumulate around some cone nuclei (Figure 1G) suggesting delayed ML-opsin synthesis compared to the wild type (Figure 1B, left panel). At P15 (Figure 1H, left panel), *Nphp5$^{+/+}$; Nrl$^{-/-}$* COS develop and reach full-length between 1 and 2 months (Figure 1I,J, left panel). In the *Nphp5$^{-/-}$; Nrl$^{-/-}$* double-knockout mutants, cone outer segments never develop, and ML-opsin accumulates in the inner segments and cell bodies (Figure 1H–M, right panels). At 23 months, a significant accumulation of ML-opsin in the cone ONL and the OPL is observed (Figure 1L, right panel). The *Nphp5$^{-/-}$; Nrl$^{-/-}$* cone inner segments and the *Nphp5$^{+/+}$; Nrl$^{-/-}$* cone outer segments survived up to 6 months, and the ONL of cone-only mutants and controls is slightly reduced at this age (Figure 1M, graph Figure 1N). The unexpected survival of mutant cones that are unable to receive and transduce light suggests a relatively long interval to develop AAV vectors expressing NPHP5 to restart cone ciliogenesis and rescue function.

Rescue of ciliogenesis with viral expression of FL-cNPHP5 in the cone-only retina: The vector scGRK1-FL-cNPHP5 (Figure 2A) expresses full-length canine NPHP5 (FL-cNPHP5) with an N-terminal Flag-tag (Flag) under the control of the human GRK1 promoter directing expression to rods and cones. Canine NPHP5 is 88% identical with human and mouse NPHP5 (93% sequence similarity), and the three polypeptides are of identical length, suggesting an identical function (Figure 2B,C). The calmodulin-binding IQ motifs are essentially identical (Figure 2B). The vector was packaged into a self-complementary (Y733F;P4211) capsid mutant of AAV2/8 virus that was injected into the subretinal space at P12–P15, and the eyes were harvested 6 weeks post-injection. A total of five each of single-knockout *Nphp5$^{+/-}$* and *Nphp5$^{-/-}$* and double-knockout *Nphp5$^{+/-}$; Nrl$^{-/-}$* and *Nphp5$^{-/-}$; Nrl$^{-/-}$* mice were injected. The heterozygous controls were comparable to the wild-type controls suggesting haplosufficiency (reported in this and a previous study [30].

There were no statistically significant differences in the a- and b-wave responses in the photopic ERGs of the untreated and treated *Nphp5$^{+/-}$; Nrl$^{-/-}$* retinas at two different light intensities (1.4 Log cd·s·m^{-2} and 2.4 Log cd·s·m^{-2}), indicating an intact retina/RPE after the subretinal virus injection (Figure 3A,B). The uninjected *Nphp5$^{-/-}$; Nrl$^{-/-}$* double-knockout retina shows no photopic response even at high light intensity (2.4 Log cd·s·m^{-2}) indicating nonfunctional cone photoreceptors (Figure 3A–D). Treatment with FL-cNPHP5 AAV (AAV^{+}) rescues cone function in mutant animals as there is a 30% increase in photopic ERG (at light intensities of 0.9 Log cd·s·m^{-2} and higher) relative to that for the untreated mice (Figure 3A–D). The statistically significant increase in the photopic b-wave amplitude (Figure 3C) and the absence of the scotopic a-wave are consistent with a cone-only retina.

Viral expression of Flag-tagged FL-cNPHP5 in Nphp5$^{-/-}$; Nrl$^{-/-}$ COS: In the virus-injected *Nphp5$^{+/-}$* retina containing

a stable ONL and exhibiting no degeneration at 6 weeks post-injection, Flag-tagged FL-cNPHP5 (red, Figure 4A, right panel) is detectable in the proximal outer segments. The inset in the figure shows photoreceptor cells in which centrioles and a connecting cilium (CC), identified with transgenic EGFP-CETN2 (*eCetn2*$^{+}$) expression, are recognized (green). In the treated *Nphp5*$^{-/-}$ retina (Figure 4B, right panel), expression of Flag-tagged FL-cNPHP5 is detectable, and the mutant ONL has recovered slightly to two layers of nuclei (or is not as degenerated as the 2-month-old untreated *Nphp5*$^{-/-}$ retina; Figure 4B, left panel). At 2 months, the *Nphp5*$^{-/-}$ photoreceptors are completely degenerated (Figure 4B, left panel; Figure 1E, right panel).

The uninjected and treated (AAV^{+}) *Nphp5*$^{+/-}$; *Nrl*$^{-/-}$ retina shows normal ciliogenesis (Figure 4C), while the treated heterozygotes show strong expression of Flag-tagged FL-cNPHP5 (red) in the proximal COS. In the uninjected *Nphp5*$^{-/-}$; *Nrl*$^{-/-}$ retina, a connecting cilium does not develop (Figure 4D, left panels), while in the treated retina, Flag-tagged FL-cNPHP5 accumulates in the proximal outer segments (Figure 4D, right panels), resembling the localization of Flag-cNPHP5 in the control retina (Figure 4C, right panels) and suggesting the initiation of normal ciliogenesis.

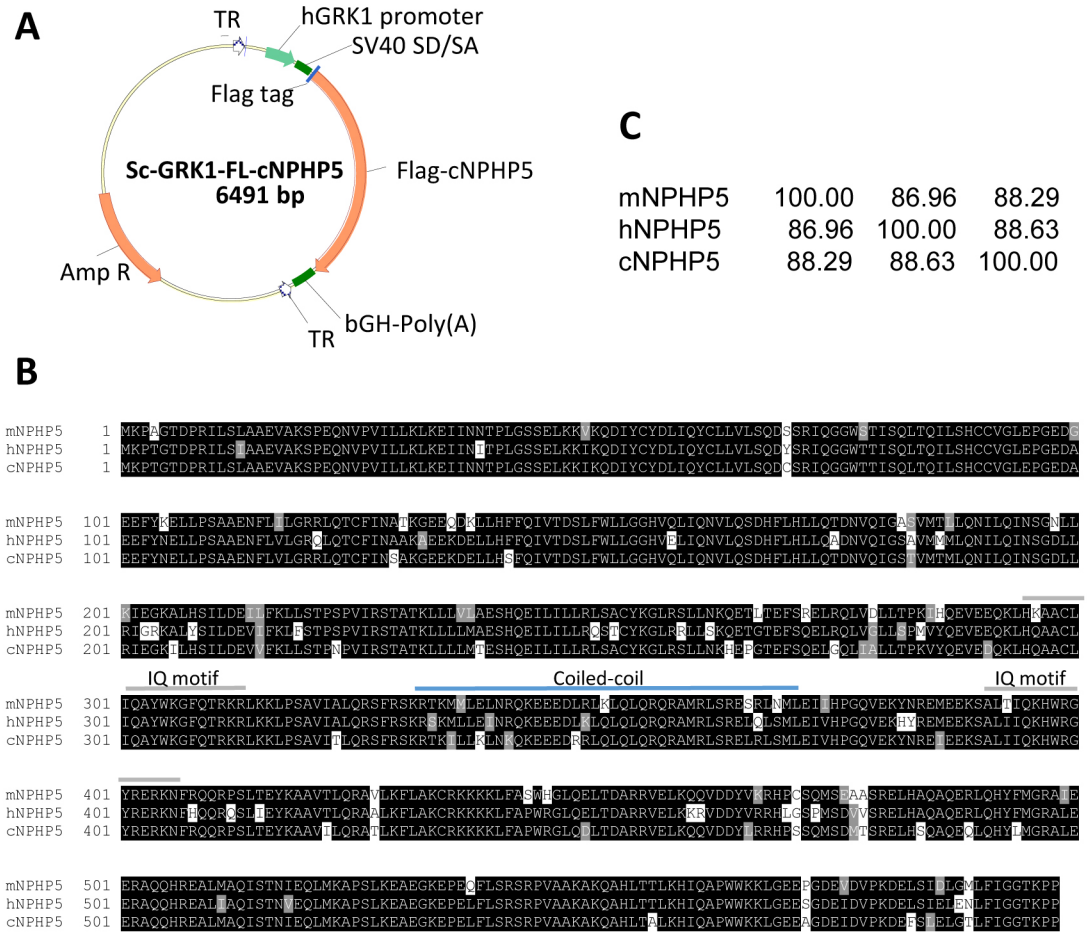

Figure 2. Shuttle vector and sequence alignment of mouse, human and canine *NPHP5*. **A**: scAAV8 shuttle vector used for preparation of the AAV. N-terminally Flag-tagged full-length (FL) canine NPHP5 (cNPHP5) is expressed under the control of the human GRK1 promoter. TR, terminal repeats; SV40 SD/SA, SV40 splice donor/splice acceptor; bGH-Poly(A), bovine growth hormone polyA signal. **B**: Sequence alignment of mouse (m), human (h), and canine (c) IQCB1/NPHP5 polypeptides. Identical residues are white on black background; conservative substitutions are white on gray background. Divergent residues are printed black. The alignment shows identical length (no gaps) and high conservation throughout. **C**: Identical residues among the sequences (%) calculated with Clustal W alignment of the three sequences.

This effect is reproducible in four additional animals. The results indicate the presence of a connecting cilium and a rudimentary outer segment in the *Nphp5*$^{-/-}$; *Nrl*$^{-/-}$ retina formed upon injection of a virus expressing full-length cNPHP5.

We examined the spread of the injected virus by analyzing the expression of cone PDE6 (cPDE) in *Nphp5*$^{-/-}$; *Nrl*$^{-/-}$ whole transverse sections. Uninjected heterozygous controls on the *Nrl*$^{-/-}$ background show uniform cone PDE6 expression in the cone outer segments, both nasally and temporally (Figure 4E). In the untreated *Nphp5*$^{-/-}$; *Nrl*$^{-/-}$ retina (Figure 4F), in contrast, cone PDE6 is undetectable (the few red dots of Figure 4F are RPE artifacts), as no outer segments form, and cone PDE6 is degraded. In the treated heterozygous controls, cone PDE6 is present in the OS layer, both nasally and temporally (Figure 4G). In the treated double-knockouts, cone PDE6 can be detected only on the nasal side near the point of injection (white asterisk, Figure 4H).

Evidence of establishing cone axonemes and COS in treated Nphp5$^{-/-}$*; Nrl*$^{-/-}$ *retina:* As a measure of the formation of outer segments, we selected an antibody directed against retinitis pigmentosa protein 1 (RP1), a microtubule-associated protein

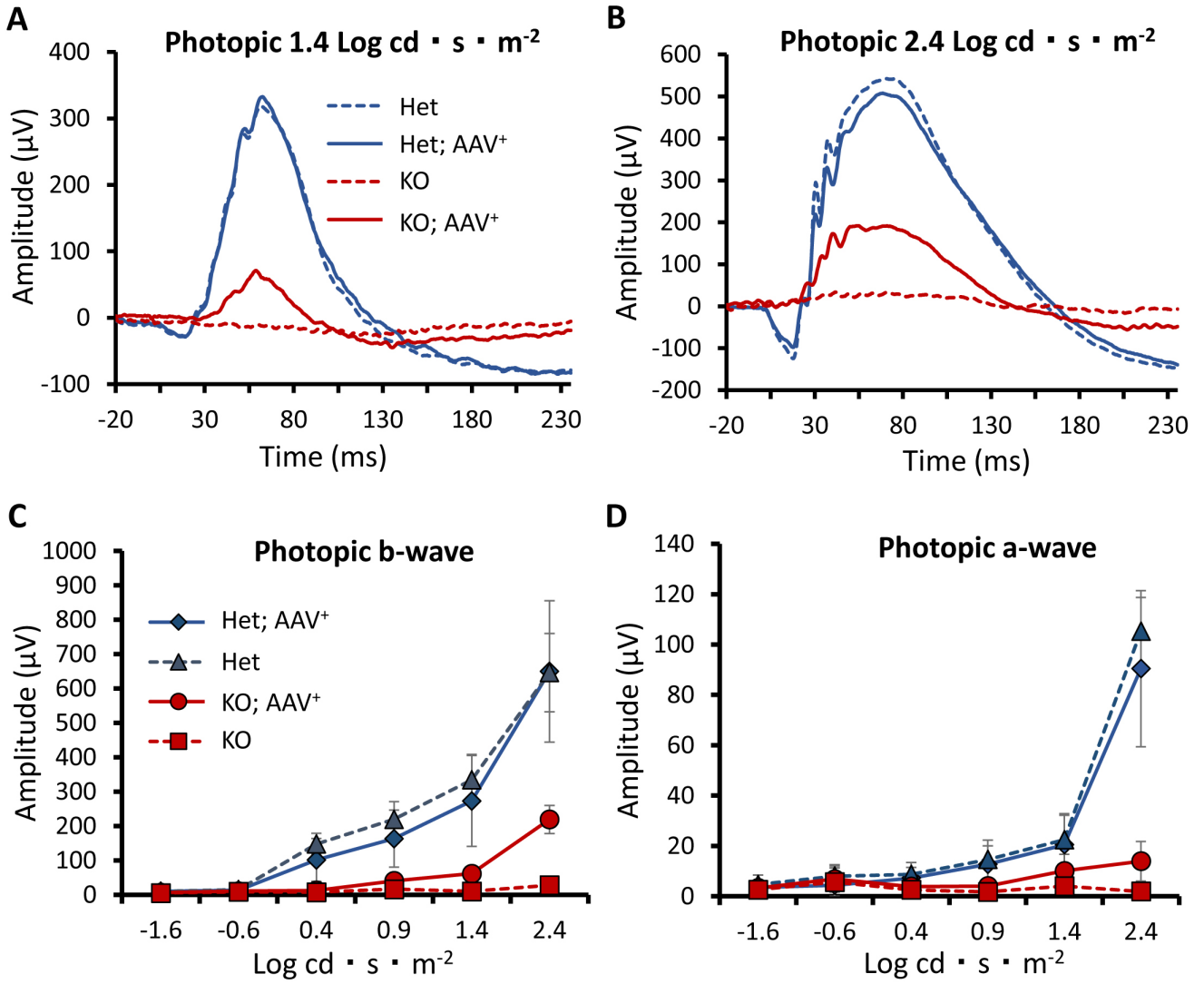

Figure 3. Functional rescue of cone-only *Nphp5*$^{-/-}$ retina. **A, B**: Photopic electroretinography (ERG) traces (n=5) of 2-month-old untreated and treated *Nphp5*$^{+/-}$; *Nrl*$^{-/-}$ and *NPHP5*$^{-/-}$; *Nrl*$^{-/-}$ at 1.4 Log cd*s*m^{-2} (**A**) and 2.4 Log cd*s*m^{-2} (**B**). **C, D**: Photopic ERG b-wave (**C**) and photopic ERG a-wave (**D**) amplitudes (n=5) of untreated and treated *Nphp5*$^{+/-}$; *Nrl*$^{-/-}$ and *NPHP5*$^{-/-}$; *Nrl*$^{-/-}$ mice (n=5) as a function of flash intensity (Log cd*s*m^{-2}).

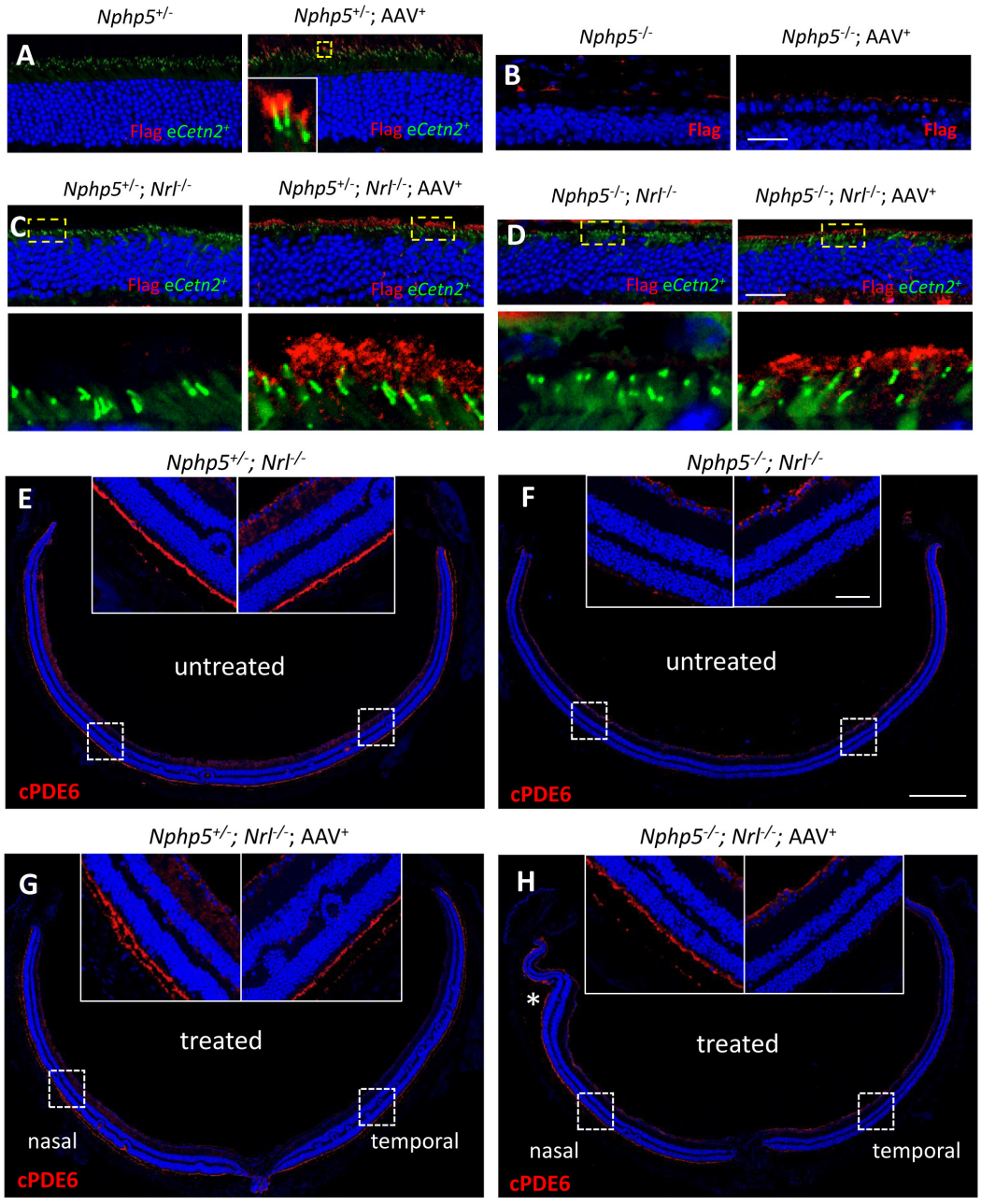

Figure 4. Rescue of ciliogenesis with scAAV8 vector expressing cNPHP5, detected with immunohistochemistry using anti-Flag antibody. **A**–**D**: Retina cryosections from *Nphp5*$^{+/-}$; *Nrl*$^{-/-}$ (**A**), *Nphp5*$^{+/-}$; *Nrl*$^{-/-}$ treated with self-complementary adenoassociated virus 8 (scAAV8)-cNPHP5 (AAV^{+}; **B**), *Nphp5*$^{-/-}$; *Nrl*$^{-/-}$ (**C**), and *Nphp5*$^{-/-}$; *Nrl*$^{-/-}$; AAV^{+} (**D**) were probed with monoclonal anti-Flag antibody (red). Lower panels show enlargements of hatched boxes. All mice expressed the *Egfp-Cetn2*$^{+}$ transgene (*eCetn2*$^{+}$, green) which specifically labels centrioles and transition zones. Please note that *Egfp-Cetn2*$^{+}$ binding to the lumen of *NPHP5*$^{-/-}$; *Nrl*$^{-/-}$ centrioles is impaired resulting in dispersion to the inner segments. OS, outer segment; CC, connecting cilium; ONL, outer nuclear layer. Scale bar, 20 µm. **E**–**H**: Cone PDE6 expression profile in untreated and treated (AAV^{+}) retinas. *Nphp5*$^{+/-}$; *Nrl*$^{-/-}$ (**E**), *Nphp5*$^{-/-}$; *Nrl*$^{-/-}$ (**F**), *Nphp5*$^{+/-}$; *Nrl*$^{-/-}$; AAV^{+} (**G**), and *Nphp5*$^{-/-}$; *Nrl*$^{-/-}$; AAV^{+} retina whole cryosections (**H**) were probed with anticone PDE6 (cPDE) antibody (red). Note the absence of expression in the double-knockout (**F**) and partial expression of cone PDE6 nasally in the treated retina. Indentation *, point of injection. Cryosections in **A**, **C**, and **D** are from mice on the *Egfp-Cetn2*$^{+}$ background. Scale bar, 200 µm; enlargement, 50 µm.

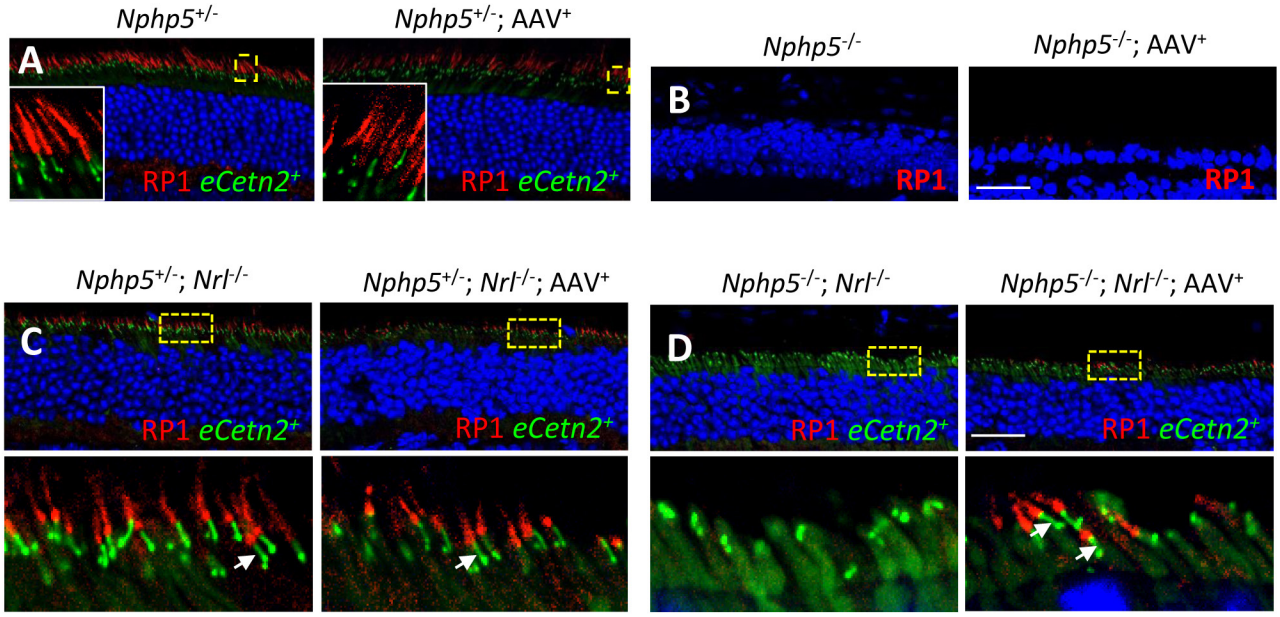

Figure 5. scAAV8-FL-cNPHP5 treatment (AAV+) reinitiates cone ciliogenesis in *Nphp5*$^{-/-}$; *Nrl*$^{-/-}$ retina. **A, B**: Immunohistochemistry of untreated (left) and treated (adenoassociated virus (AAV+), right) retina cryosections from *Nphp5*$^{+/-}$ (A), and *Nphp5*$^{-/-}$ mice (B). **C, D**: Immunohistochemistry of untreated (left) and treated (right) retina cryosections from *Nphp5*$^{+/-}$; *Nrl*$^{-/-}$ (**C**) and *Nphp5*$^{-/-}$; *Nrl*$^{-/-}$ (**D**) mice. Mutant mice were kept on the *Egfp-Cetn2*$^{+}$ background (e*Cetn2*$^{+}$, green), and sections were probed with anti-RP1 antibody (red) to label the developing axoneme. Lower panels are enlargements of hatched boxes. Note the presence of the axoneme (red), connecting cilium (CC, green, white arrows), and mother and daughter centrioles (green dots) in the controls (**C**); the absence of axoneme and CC in the double-knockout mice (**D**, left panel); and reemergence of the axoneme, CC, and centrioles in the treated double-knockout mice (**D**, right panel). Cryosections in **A**–**J** are from mice on the *Egfp-Cetn2*$^{+}$ background. Scale bar, 20 µm.

that interacts with proximal microtubules of the axoneme, but not the doublet microtubule array of the transition zone (the connecting cilium) or basal body [48]. In the untreated and treated *Nphp5*$^{+/-}$ retinas with normally developed photoreceptors (Figure 5A), RP1 (red) labels the proximal OS of rods and cones, nicely visible in the enlarged insets of Figure 5A. In the treated *Nphp5*$^{-/-}$ retina (Figure 5B, right panel), a functional CC and a proximal OS are absent as the degeneration is fast.

The RP1 antibody labels the axoneme in the treated and untreated undegenerated *Nphp5*$^{+/-}$*; Nrl*$^{-/-}$ retinas (Figure 5C). In the untreated *Nphp5*$^{-/-}$*; Nrl*$^{-/-}$ retina, the axoneme and the outer segments are absent (Figure 5D, left panel). Treatment with scAAV8-cNPHP5 rebuilds the transition zone and the axoneme of mutant mice (Figure 5D, right panel). Enlargements of the treated *Nphp5*$^{-/-}$*; Nrl*$^{-/-}$ retina (Figure 5D, lower panel) reveal that each cone basal body extends a transition zone (white arrows) and an axoneme (red). Lower panels of the untreated *Nphp5*$^{-/-}$*; Nrl*$^{-/-}$ retina (Figure 5D, left panel) show only basal bodies and daughter centrioles with *eCetn2*$^{+}$ dispersion within the distal inner segment. Accumulation of soluble *eCetn2*$^{+}$ in the *Nphp5*$^{-/-}$*; Nrl*$^{-/-}$ inner segments is characteristic of other mouse models that are unable to form axonemes and transition zones [45].

COS phototransduction proteins relocate to the treated Nphp5$^{-/-}$*; Nrl*$^{-/-}$ *retina:* Cone pigments (red) localize normally to relatively disorganized membranes of the treated and untreated *Nphp5*$^{+/-}$*; Nrl*$^{-/-}$ outer segments (Figure 6A,C, and lower panel enlargements) and do not colocalize with *eCetn2*$^{+}$ (green). In the untreated *Nphp5*$^{-/-}$*; Nrl*$^{-/-}$ retina, S-opsin and ML-opsin mislocalize within the inner segments and the ONL due to the total absence of outer segments (Figure 6B,D, left and lower panels). Treatment of the *Nphp5*$^{-/-}$*; Nrl*$^{-/-}$ retina with Flag-tagged FL-cNPHP5 enables formation of outer segments and therefore, allows correct trafficking of cone pigments to the outer segments (Figure 6B,D, right and lower panels).

Cone PDE6 and cone transducin (cTα and cTβγ) traffic normally to the untreated and treated *Nphp5*$^{+/-}$*; Nrl*$^{-/-}$ cone outer segments where phototransduction occurs (Figure 6,

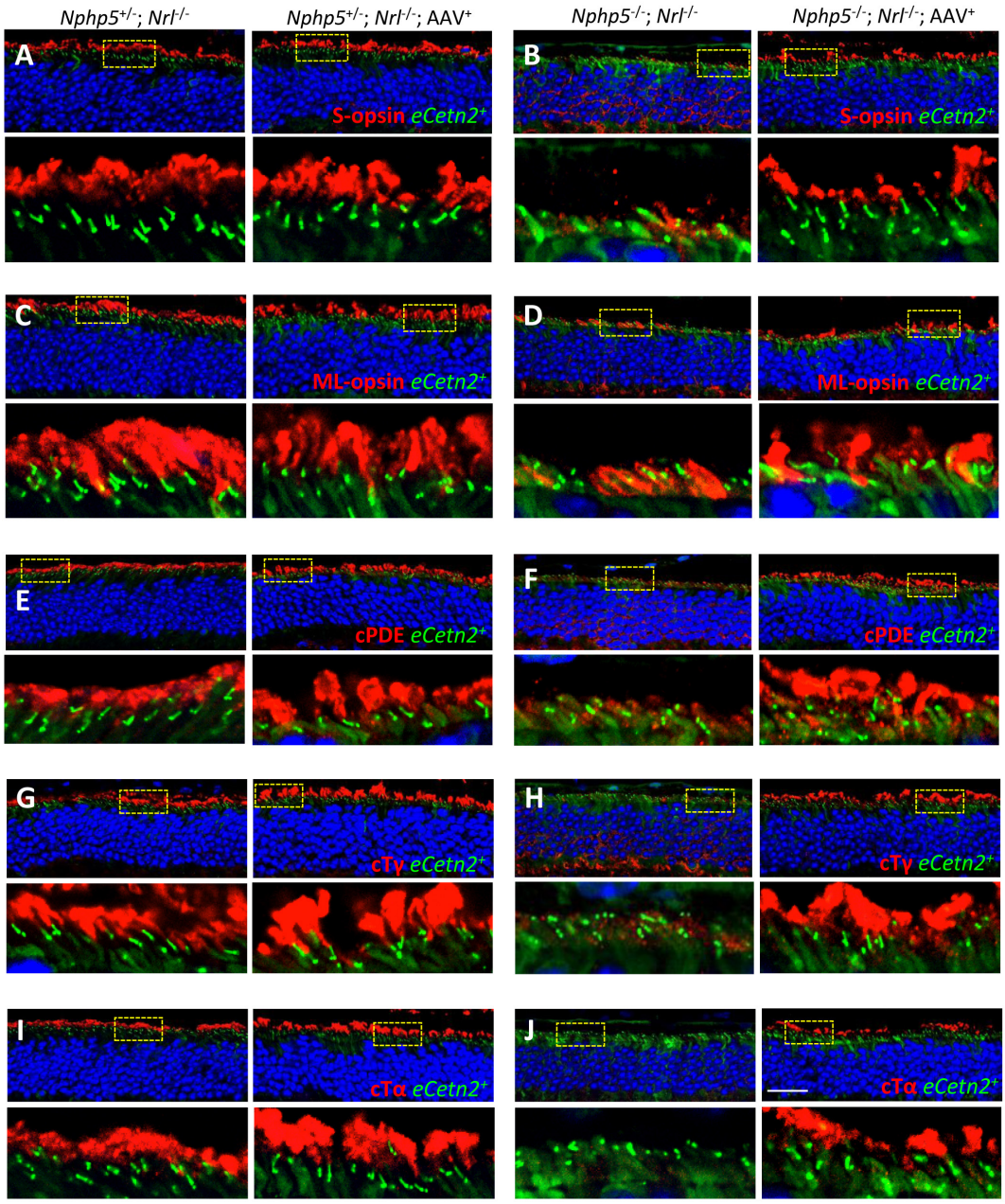

Figure 6. COS proteins restored to the outer segments of treated *Nphp5*$^{-/-}$; *Nrl*$^{-/-}$ mice. **A**–**J**: Immunohistochemistry of retina cryosections from untreated (left) and treated (right) *Nphp5*$^{+/-}$; *Nrl*$^{-/-}$ (**A**, **C**, **E**, **G**, and **I**) and *Nphp5*$^{-/-}$; *Nrl*$^{-/-}$ (**B**, **D**, **F**, **H**, and **J**) mice. Cryosections were probed with antibodies directed against S-opsin (**A**, **B**), ML-opsin (**C**, **D**), cone PDE6 (**E**, **F**), cone transducin-γ (**G**, **H**), and cone transducin-α (**I**, **J**). Lower panels (**A**–**J**) show enlargements of dashed boxes (yellow); all sections were from mice expressing *Egfp-Cetn2*$^{+}$ (e*Cetn2*$^{+}$, green). Scale bar, 20 µm. Note the absence of cone phototransduction components in the untreated double-knockout (**B**, **D**, **F**, **H**, and **J**, left panels) and partial restoration following treatment (**B**, **D**, **F**, **H**, and **J**, right panels).

E,G,I). In the untreated *Nphp5*$^{-/-}$*; Nrl*$^{-/-}$ retina, phototransduction proteins mislocalize to the inner segments and the ONL, as outer segments fail to form, and are degraded (Figure 6F,H,J, left panels). Treatment with scAAV8 expressing FL-cNPHP5 reinitiates development of the CC and formation of rudimentary outer segments, such that cPDE6, cTα, and cTγ relocate to the outer segments (Figure 6F,H,J, right panels).

DISCUSSION

Nphp5$^{-/-}$ mice are blind at eye opening (P12), a phenotype resembling Leber congenital amaurosis. Photoreceptors deficient in NPHP5 are unable to form connecting cilia and outer segments, the site of phototransduction. Mutant rods degenerate rapidly although a single row of nuclei, presumably those of cones, survives much longer (Figure 1E, right panel) and [30]. We showed that in *Nphp5*$^{-/-}$*; Nrl*$^{-/-}$ (cone-only) mice, cone nuclei and inner segments are able to survive for more than 6 months (Figure 1N). The thickness of the cone double-knockout ONL persists, similarly as observed in the *Cep290/Nphp6*$^{rd16/rd16}$*/Nrl* double-knockout retina [36]. *Nphp5*$^{-/-}$*; Nrl*$^{-/-}$ cones continue to express cone pigments without triggering cone degeneration (Figure 1G–M). With the application of AAV gene replacement therapy with a vector expressing canine NPHP5 (Figure 2), transition zones and cilia in *Nphp5*$^{-/-}$*; Nrl*$^{-/-}$ cones were reestablished (Figures 4–6), and cone outer segment proteins trafficked normally to the outer segment membranes (Figure 6). Six weeks postinjection, ERG of the AAV-treated retina showed a photopic b-wave roughly one third of the control (Figure 3), suggesting a significant number of cones had been rescued and were functional.

Photoreceptor ciliogenesis in *Nphp5* germline knockouts was arrested at a stage when basal bodies are docked to the cortex of the inner segments but are unable to generate an axoneme and functional transition zones [30]. The most obvious defect is the formation of a few stunted transition zones to which amorphous bags lacking discernible disc structures are attached [30]. As shown in Figure 4D and Figure 5D, the association of CETN2 with centrioles is impaired resulting in solubilization and dispersion of CETN2 to the inner segments. Similar results were observed in the Arl3−/− mouse which is unable to form an axoneme [45]. In wild-type mice, docking of the basal body and generation of the transition zone consisting of nine doublet microtubules takes place around P3 and P4. Around P6 and P7, an axoneme emerges, and the first stacks of discs are synthesized. The formation of the outer segments is complete at P21 [49,50]. Inability to form transition zones has been observed in various retina-specific knockouts, including KIF3a, the obligatory subunit of heterotrimeric kinesin-2 [51] and the small GTPases, ARL3 and ARL13b [45,52]. Absence of ARL3-GTP has been linked to defects in photoreceptor intraflagellar transport (IFT), a pathway essential for the formation of the transition zone and axonemes. The nearly identical photoreceptor phenotypes of *Nphp5*$^{-/-}$, ^{ret}*Kif3a*$^{-/-}$, and ^{ret}*Arl3*$^{-/-}$ mice raise the possibility that NPHP5 participates in some aspect of IFT.

Based on tissue culture experiments with IMCD3, HEK293, and RPE cell lines, NPHP5 and Cep290/NPHP6 are known to form a complex localizing to the transition zone, possibly being part of a gate complex. With the use of transmission electron microscopy of the mouse retina, NPHP6 was shown to be part of the Y linkers connecting the microtubule doublets with the ciliary membrane [53]. *Cep290*$^{-/-}$ photoreceptor basal bodies formed but did not dock to the apical cell membrane and therefore, never formed a transition zone. According to immunohistochemistry, NPHP5 and NPHP6 also locate to the proximal outer segments [30,32]. *Cep290* germline knockouts with deletions of exons 1–4 died before weaning due to the development of syndromic ciliopathy and hydrocephalus [53], a phenotype much stronger than that seen with germline *Nphp5* deletions. The homozygous mutants exhibit a Joubert syndrome (JBTS)/ciliopathy phenotype, including retinal degeneration, cerebral abnormalities, and progressive cystic kidney disease consistent with the human phenotype. Obviously, the in vivo functions of NPHP5 and NPHP6 are distinct and not complementary.

In other mammalian species, *Nphp5*$^{-/-}$ ciliary phenotypes differ, perhaps because stable truncated proteins are generated. In a *Crd2* canine animal model (American pit bull terrier) with a p.S319fsX12 premature truncation of NPHP5, one of the two IQ calmodulin binding motifs and the two central coiled-coil motifs are present in the truncated protein. The mutant photoreceptors form a sensory cilium but are nearly nonfunctional. At 6 weeks, the ONL looks normal, and the rod ERG is absent, but mutant dogs show a weak photopic b-wave suggesting that mutant cones survive longer [38,54]. A 2 bp deletion in exon 13 of NPHP5 in an African black-footed cat (*Felix nigripes*, Fnig) truncates NPHP5 (p.L428*), removing 170 amino acids at the C-terminal of NPHP5, including Cep290 interaction sites. The mutation is associated with early onset non-syndromic progressive retinal atrophy (PRA) where the ERG is non-recordable. It is unclear at which point ciliogenesis is interrupted in the cat model.

Gene replacement therapies for patients with Senior-Løken syndrome or other syndromic ciliopathies are currently not available, mostly because gene delivery to internal organs like kidneys is challenging, and AAV gene delivery is restricted by size. Furthermore, the application

window is often short as organs degenerate before the gene of interest can be expressed. Fortunately, this laboratory-generated mouse model and naturally occurring canine and cat models harboring NPHP5 gene defects do not develop nephronophthisis, allowing researchers to test retina gene replacement strategies in an otherwise healthy and fertile animal. These results show that *Nphp5*$^{-/-}$ cones are initially viable, and the cone-only mutant mice provide an extended time interval during which mutant cones can be rescued with viral expression of NPHP5. As cones are most important for daylight vision, these results provide hope for patients with NPHP5-SLS that visual defects may be ameliorated in the future with gene-based therapies.

ACKNOWLEDGMENTS

This work was supported in part by NIH grants R01EY008123 (WB), R01EY019298 (WB), P30EY014800 (NEI core grant), R01EY017549; unrestricted grants to the University of Utah Department of Ophthalmology from Research to Prevent Blindness (RPB; New York). WB is the recipient of an RPB Senior Investi-gator award, a RPB Nelson Trust Award, and an award from the Retina Research Foundation (Alice McPherson, MD), Houston, TX.

REFERENCES

1. Shiba D, Yokoyama T. The ciliary transitional zone and nephrocystins. Differentiation 2012; 83:S91-6. [PMID: 22169048].
2. Sang L, Miller JJ, Corbit KC, Giles RH, Brauer MJ, Otto EA, Baye LM, Wen X, Scales SJ, Kwong M, Huntzicker EG, Sfakianos MK, Sandoval W, Bazan JF, Kulkarni P, Garcia-Gonzalo FR, Seol AD, O'Toole JF, Held S, Reutter HM, Lane WS, Rafiq MA, Noor A, Ansar M, Devi AR, Sheffield VC, Slusarski DC, Vincent JB, Doherty DA, Hildebrandt F, Reiter JF, Jackson PK. Mapping the NPHP-JBTS-MKS protein network reveals ciliopathy disease genes and pathways. Cell 2011; 145:513-28. [PMID: 21565611].
3. Fliegauf M, Horvath J. von SC, Olbrich H, Muller D, Thumfart J, Schermer B, Pazour GJ, Neumann HP, Zentgraf H, Benzing T, Omran H: Nephrocystin specifically localizes to the transition zone of renal and respiratory cilia and photoreceptor connecting cilia. J Am Soc Nephrol 2006; 17:2424-33. [PMID: 16885411].
4. Winkelbauer ME, Schafer JC, Haycraft CJ, Swoboda P, Yoder BK. The C. elegans homologs of nephrocystin-1 and nephrocystin-4 are cilia transition zone proteins involved in chemosensory perception. J Cell Sci 2005; 118:5575-87. [PMID: 16291722].
5. Doherty D. Joubert syndrome: insights into brain development, cilium biology, and complex disease. Semin Pediatr Neurol 2009; 16:143-54. [PMID: 19778711].
6. Sampathkumar K, Sooraj YS, Karunakaran N, Ganesh R, Mahaldar AR. Joubert syndrome. Kidney Int 2008; 74:1222-[PMID: 18854854].
7. Parisi MA, Doherty D, Chance PF, Glass IA. Joubert syndrome (and related disorders) (OMIM 213300). Eur J Hum Genet 2007; 15:511-21. [PMID: 17377524].
8. Valente EM, Silhavy JL, Brancati F, Barrano G, Krishnaswami SR, Castori M, Lancaster MA, Boltshauser E, Boccone L, Al-Gazali L, Fazzi E, Signorini S, Louie CM, Bellacchio E, Bertini E, Dallapiccola B, Gleeson JG. Mutations in CEP290, which encodes a centrosomal protein, cause pleiotropic forms of Joubert syndrome. Nat Genet 2006; 38:623-5. [PMID: 16682970].
9. Sayer JA, Otto EA, O'Toole JF, Nurnberg G, Kennedy MA, Becker C, Hennies HC, Helou J, Attanasio M, Fausett BV, Utsch B, Khanna H, Liu Y, Drummond I, Kawakami I, Kusakabe T, Tsuda M, Ma L, Lee H, Larson RG, Allen SJ, Wilkinson CJ, Nigg EA, Shou C, Lillo C, Williams DS, Hoppe B, Kemper MJ, Neuhaus T, Parisi MA, Glass IA, Petry M, Kispert A, Gloy J, Ganner A, Walz G, Zhu X, Goldman D, Nurnberg P, Swaroop A, Leroux MR, Hildebrandt F. The centrosomal protein nephrocystin-6 is mutated in Joubert syndrome and activates transcription factor ATF4. Nat Genet 2006; 38:674-81. [PMID: 16682973].
10. Utsch B, Sayer JA, Attanasio M, Pereira RR, Eccles M, Hennies HC, Otto EA, Hildebrandt F. Identification of the first AHI1 gene mutations in nephronophthisis-associated Joubert syndrome. Pediatr Nephrol 2006; 21:32-5. [PMID: 16240161].
11. Ronquillo CC, Bernstein PS, Baehr W. Senior-Loken syndrome: A syndromic form of retinal dystrophy associated with nephronophthisis. Vision Res 2012; 75:88-97. [PMID: 22819833].
12. Omran H, Sasmaz G, Haffner K, Volz A, Olbrich H, Melkaoui R, Otto E, Wienker TF, Korinthenberg R, Brandis M, Antignac C, Hildebrandt F. Identification of a gene locus for Senior-Loken syndrome in the region of the nephronophthisis type 3 gene. J Am Soc Nephrol 2002; 13:75-9. [PMID: 11752023].
13. Schuermann MJ, Otto E, Becker A, Saar K, Ruschendorf F, Polak BC, Ala-Mello S, Hoefele J, Wiedensohler A, Haller M, Omran H, Nurnberg P, Hildebrandt F. Mapping of gene loci for nephronophthisis type 4 and Senior-Loken syndrome, to chromosome 1p36. Am J Hum Genet 2002; 70:1240-6. [PMID: 11920287].
14. Baala L, Romano S, Khaddour R, Saunier S, Smith UM, Audollent S, Ozilou C, Faivre L, Laurent N, Foliguet B, Munnich A, Lyonnet S, Salomon R, Encha-Razavi F, Gubler MC, Boddaert N. de LP, Johnson CA, Vekemans M, Antignac C, Attie-Bitach T: The Meckel-Gruber syndrome gene, MKS3, is mutated in Joubert syndrome. Am J Hum Genet 2007; 80:186-94. [PMID: 17160906].
15. Kyttala M, Tallila J, Salonen R, Kopra O, Kohlschmidt N, Paavola-Sakki P, Peltonen L, Kestila M. MKS1, encoding a component of the flagellar apparatus basal body proteome,

is mutated in Meckel syndrome. Nat Genet 2006; 38:155-7. [PMID: 16415886].

16. Bialas NJ, Inglis PN, Li C, Robinson JF, Parker JD, Healey MP, Davis EE, Inglis CD, Toivonen T, Cottell DC, Blacque OE, Quarmby LM, Katsanis N, Leroux MR. Functional interactions between the ciliopathy-associated Meckel syndrome 1 (MKS1) protein and two novel MKS1-related (MKSR) proteins. J Cell Sci 2009; 122:611-24. [PMID: 19208769].

17. Consugar MB, Kubly VJ, Lager DJ, Hommerding CJ, Wong WC, Bakker E, Gattone VH, Torres VE, Breuning MH, Harris PC. Molecular diagnostics of Meckel-Gruber syndrome highlights phenotypic differences between MKS1 and MKS3. Hum Genet 2007; 121:591-9. [PMID: 17377820].

18. Forsythe E, Beales PL. Bardet-Biedl syndrome. Eur J Hum Genet 2013; 21:8-13. [PMID: 22713813].

19. Yen HJ, Tayeh MK, Mullins RF, Stone EM, Sheffield VC, Slusarski DC. Bardet-Biedl syndrome genes are important in retrograde intracellular trafficking and Kupffer's vesicle cilia function. Hum Mol Genet 2006; 15:667-77. [PMID: 16399798].

20. Blacque OE, Leroux MR. Bardet-Biedl syndrome: an emerging pathomechanism of intracellular transport. Cell Mol Life Sci 2006; 63:2145-61. [PMID: 16909204].

21. Jiang ST, Chiou YY, Wang E, Chien YL, Ho HH, Tsai FJ, Lin CY, Tsai SP, Li H. Essential role of nephrocystin in photoreceptor intraflagellar transport in mouse. Hum Mol Genet 2009; 18:1566-77. [PMID: 19208653].

22. Won J. Marin de EC, Smith RS, Hicks WL, Edwards MM, Longo-Guess C, Li T, Naggert JK, Nishina PM: NPHP4 is necessary for normal photoreceptor ribbon synapse maintenance and outer segment formation, and for sperm development. Hum Mol Genet 2011; 20:482-96. [PMID: 21078623].

23. Estrada-Cuzcano A, Koenekoop RK, Coppieters F, Kohl S, Lopez I, Collin RW, De Baere EB, Roeleveld D, Marek J, Bernd A, Rohrschneider K, Van den Born LI, Meire F, Maumenee IH, Jacobson SG, Hoyng CB, Zrenner E, Cremers FP, den Hollander AI. IQCB1 mutations in patients with leber congenital amaurosis. Invest Ophthalmol Vis Sci 2011; 52:834-9. [PMID: 20881296].

24. Moradi P, Davies WL, Mackay DS, Cheetham ME, Moore AT. Focus on molecules: centrosomal protein 290 (CEP290). Exp Eye Res 2011; 92:316-7. [PMID: 20493186].

25. Menotti-Raymond M, David VA, Schaffer AA, Stephens R, Wells D, Kumar-Singh R, O'Brien SJ, Narfstrom K. Mutation in CEP290 discovered for cat model of human retinal degeneration. J Hered 2007; 98:211-20. [PMID: 17507457].

26. den Hollander AI, Koenekoop RK, Yzer S, Lopez I, Arends ML, Voesenek KE, Zonneveld MN, Strom TM, Meitinger T, Brunner HG, Hoyng CB, Van den Born LI, Rohrschneider K, Cremers FP. Mutations in the CEP290 (NPHP6) gene are a frequent cause of Leber congenital amaurosis. Am J Hum Genet 2006; 79:556-61. [PMID: 16909394].

27. Patil H, Tserentsoodol N, Saha A, Hao Y, Webb M, Ferreira PA. Selective loss of RPGRIP1-dependent ciliary targeting of NPHP4, RPGR and SDCCAG8 underlies the degeneration of photoreceptor neurons. Cell Death Dis 2012; 3:e355-[PMID: 22825473].

28. Otto EA, Hurd TW, Airik R, Chaki M, Zhou W, Stoetzel C, Patil SB, Levy S, Ghosh AK, Murga-Zamalloa CA. van RJ, Letteboer SJ, Sang L, Giles RH, Liu Q, Coene KL, Estrada-Cuzcano A, Collin RW, McLaughlin HM, Held S, Kasanuki JM, Ramaswami G, Conte J, Lopez I, Washburn J, Macdonald J, Hu J, Yamashita Y, Maher ER, Guay-Woodford LM, Neumann HP, Obermuller N, Koenekoop RK, Bergmann C, Bei X, Lewis RA, Katsanis N, Lopes V, Williams DS, Lyons RH, Dang CV, Brito DA, Dias MB, Zhang X, Cavalcoli JD, Nurnberg G, Nurnberg P, Pierce EA, Jackson PK, Antignac C, Saunier S, Roepman R, Dollfus H, Khanna H, Hildebrandt F: Candidate exome capture identifies mutation of SDCCAG8 as the cause of a retinal-renal ciliopathy. Nat Genet 2010; 42:840-50. [PMID: 20835237].

29. Collin GB, Won J, Hicks WL, Cook SA, Nishina PM, Naggert JK. Meckelin is necessary for photoreceptor intraciliary transport and outer segment morphogenesis. Invest Ophthalmol Vis Sci 2012; 53:967-74. [PMID: 22247471].

30. Ronquillo CC, Hanke-Gogokhia C, Revelo MP, Frederick JM, Jiang L, Baehr W. Ciliopathy-associated IQCB1/NPHP5 protein is required for mouse photoreceptor outer segment formation. FASEB J 2016; 30:3400-12. [PMID: 27328943].

31. Stone EM, Cideciyan AV, Aleman TS, Scheetz TE, Sumaroka A, Ehlinger MA, Schwartz SB, Fishman GA, Traboulsi EI, Lam BL, Fulton AB, Mullins RF, Sheffield VC, Jacobson SG. Variations in NPHP5 in patients with nonsyndromic leber congenital amaurosis and Senior-Loken syndrome. Arch Ophthalmol 2011; 129:81-7. [PMID: 21220633].

32. Otto EA, Loeys B, Khanna H, Hellemans J, Sudbrak R, Fan S, Muerb U, O'Toole JF, Helou J, Attanasio M, Utsch B, Sayer JA, Lillo C, Jimeno D, Coucke P, De PA, Reinhardt R, Klages S, Tsuda M, Kawakami I, Kusakabe T, Omran H, Imm A, Tippens M, Raymond PA, Hill J, Beales P, He S, Kispert A, Margolis B, Williams DS, Swaroop A, Hildebrandt F. Nephrocystin-5, a ciliary IQ domain protein, is mutated in Senior-Loken syndrome and interacts with RPGR and calmodulin. Nat Genet 2005; 37:282-8. [PMID: 15723066].

33. Wolf MT, Hildebrandt F. Nephronophthisis. Pediatr Nephrol 2011; 26:181-94. [PMID: 20652329].

34. Hartong DT, Berson EL, Dryja TP. Retinitis pigmentosa. Lancet 2006; 368:1795-809. [PMID: 17113430].

35. den Hollander AI, Roepman R, Koenekoop RK, Cremers FP. Leber congenital amaurosis: genes, proteins and disease mechanisms. Prog Retin Eye Res 2008; 27:391-419. [PMID: 18632300].

36. Cideciyan AV, Rachel RA, Aleman TS, Swider M, Schwartz SB, Sumaroka A, Roman AJ, Stone EM, Jacobson SG, Swaroop A. Cone photoreceptors are the main targets for gene therapy of NPHP5 (IQCB1) or NPHP6 (CEP290) blindness: generation of an all-cone Nphp6 hypomorph mouse that mimics the human retinal ciliopathy. Hum Mol Genet 2011; 20:1411-23. [PMID: 21245082].

37. Oh A, Pearce JW, Gandolfi B, Creighton EK, Suedmeyer WK, Selig M, Bosiack AP, Castaner LJ, Whiting RE, Belknap EB, Lyons LA. Early-Onset Progressive Retinal Atrophy Associated with an IQCB1 Variant in African Black-Footed Cats (Felis nigripes). Sci Rep 2017; 7:43918-[PMID: 28322220].

38. Goldstein O, Mezey JG, Schweitzer PA, Boyko AR, Gao C, Bustamante CD, Jordan JA, Aguirre GD, Acland GM. IQCB1 and PDE6B mutations cause similar early onset retinal degenerations in two closely related terrier dog breeds. Invest Ophthalmol Vis Sci 2013; 54:7005-19. [PMID: 24045995].

39. Barbelanne M, Hossain D, Chan DP, Peranen J, Tsang WY. Nephrocystin proteins NPHP5 and Cep290 regulate BBSome integrity, ciliary trafficking and cargo delivery. Hum Mol Genet 2015; 24:2185-200. [PMID: 25552655].

40. Barbelanne M, Song J, Ahmadzai M, Tsang WY. Pathogenic NPHP5 mutations impair protein interaction with Cep290, a prerequisite for ciliogenesis. Hum Mol Genet 2013; 22:2482-94. [PMID: 23446637].

41. Higginbotham H, Bielas S, Tanaka T, Gleeson JG. Transgenic mouse line with green-fluorescent protein-labeled Centrin 2 allows visualization of the centrosome in living cells. Transgenic Res 2004; 13:155-64. [PMID: 15198203].

42. Mears AJ, Kondo M, Swain PK, Takada Y, Bush RA, Saunders TL, Sieving PA, Swaroop A. Nrl is required for rod photoreceptor development. Nat Genet 2001; 29:447-52. [PMID: 11694879].

43. Zhang H, Fan J, Li S, Karan S, Rohrer B, Palczewski K, Frederick JM, Crouch RK, Baehr W. Trafficking of membrane-associated proteins to cone photoreceptor outer segments requires the chromophore 11-cis-retinal. J Neurosci 2008; 28:4008-14. [PMID: 18400900].

44. Zhang H, Hanke-Gogokhia C, Jiang L, Li X, Wang P, Gerstner CD, Frederick JM, Yang Z, Baehr W. Mistrafficking of prenylated proteins causes retinitis pigmentosa 2. FASEB J 2015; 29:932-42. [PMID: 25422369].

45. Hanke-Gogokhia C, Wu Z, Gerstner CD, Frederick JM, Zhang H, Baehr W. Arf-like protein 3 (ARL3) regulates protein trafficking and ciliogenesis in mouse photoreceptors. J Biol Chem 2016; 291:7142-55. [PMID: 26814127].

46. Zolotukhin S, Byrne BJ, Mason E, Zolotukhin I, Potter M, Chesnut K, Summerford C, Samulski RJ, Muzyczka N. Recombinant adeno-associated virus purification using novel methods improves infectious titer and yield. Gene Ther 1999; 6:973-85. [PMID: 10455399].

47. Ying G, Gerstner CD, Frederick JM, Boye SL, Hauswirth WW, Baehr W. Small GTPases Rab8a and Rab11a Are Dispensable for Rhodopsin Transport in Mouse Photoreceptors. PLoS One 2016; 11:e0161236-[PMID: 27529348].

48. Liu Q, Lyubarsky A, Skalet JH, Pugh EN Jr, Pierce EA. RP1 is required for the correct stacking of outer segment discs. Invest Ophthalmol Vis Sci 2003; 44:4171-83. [PMID: 14507858].

49. Sedmak T, Wolfrum U. Intraflagellar transport proteins in ciliogenesis of photoreceptor cells. Biol Cell 2011; 103:449-66. [PMID: 21732910].

50. May-Simera H, Nagel-Wolfrum K, Wolfrum U. Cilia - The sensory antennae in the eye. Prog Retin Eye Res 2017; 60:144-80. [PMID: 28504201].

51. Jiang L, Wei Y, Ronquillo CC, Marc RE, Yoder BK, Frederick JM, Baehr W. Heterotrimeric kinesin-2 (KIF3) mediates transition zone and axoneme formation of mouse photoreceptors. J Biol Chem 2015; 290:12765-78. [PMID: 25825494].

52. Hanke-Gogokhia C, Wu Z, Sharif A, Yazigi H, Frederick JM, Baehr W. The guanine nucleotide exchange factor, Arf-like protein 13b, is essential for assembly of the mouse photoreceptor transition zone and outer segment. J Biol Chem 2017; 292:21442-56. [PMID: 29089384].

53. Rachel RA, Yamamoto EA, Dewanjee MK, May-Simera HL, Sergeev YV, Hackett AN, Pohida K, Munasinghe J, Gotoh N, Wickstead B, Fariss RN, Dong L, Li T, Swaroop A. CEP290 alleles in mice disrupt tissue-specific cilia biogenesis and recapitulate features of syndromic ciliopathies. Hum Mol Genet 2015; 24:3775-91. [PMID: 25859007].

54. Downs LM, Scott EM, Cideciyan AV, Iwabe S, Dufour V, Gardiner KL, Genini S, Marinho LF, Sumaroka A, Kosyk MS, Swider M, Aguirre GK, Jacobson SG, Beltran WA, Aguirre GD. Overlap of abnormal photoreceptor development and progressive degeneration in Leber congenital amaurosis caused by NPHP5 mutation. Hum Mol Genet 2016; 25:4211-26. [PMID: 27506978].

Articles are provided courtesy of Emory University and the Zhongshan Ophthalmic Center, Sun Yat-sen University, P.R. China. The print version of this article was created on 30 December 2018. This reflects all typographical corrections and errata to the article through that date. Details of any changes may be found in the online version of the article.